doi: 10.3969/j.issn.0490-6756.2020.06.023

雷击作用下复合材料层合板的烧蚀损伤表征及剩余强度影响因素分析

刘远飞[1], 张 驭[1], 尹俊杰[2], 周 彬[1], 惠军华[3], 彭德镇[4]
(1. 空军工程大学航空工程学院, 西安 710038; 2. 92728 部队, 上海 200040;
3. 国防科技大学信息通信学院, 西安 710106; 4. 94347 部队, 郑州 450003)

摘 要: 为表征复合材料雷击烧蚀损伤,基于唯象分析方法,建立了雷击烧蚀损伤引起的材料力学性能退化模型. 采用连续损伤力学(CDM)方法提出了复合材料雷电烧蚀损伤的三维渐进损伤退化模型,采用 Hashin 和 Yeh 分层失效准则,验证了失效点的发生情景. 根据所建立的模型和刚度矩阵渐进损伤退化模型的编码,利用 ABAQUS 软件并结合 UMAT 子程序预测了拉伸载荷下雷电烧蚀损伤复合材料层合板的残余强度,最终的仿真精度验证了该模型的有效性.

关键词: 烧蚀; 复合材料层合板; 剩余强度; 影响因素; 雷击
中图分类号: TB332 **文献标识码**: A **文章编号**: 0490-6756(2020)06-1165-12

Ablation damage characterization and tensile residual strength influence factors analysis for composite coupons subjected to lightning strike

LIU Yuan-Fei[1], *ZHANG Yu*[1], *YIN Jun-Jie*[2], *ZHOU Bin*[1], *HUI Jun-Hua*[3], *PENG De-Zhen*[4]
(1. Aeronautics Engineering College, Air Force Engineering University, Xi'an 710038, China;
2. 92728 unit, Air Force of the CPLA, Shanghai 200040, China;
3. College of Information and Communication, National University of Defense Technology, Xi'an 710106, China;
4. 94347 unit, Air Force of the CPLA, Zhengzhou 450003, China)

Abstract: To characterize composite lightning ablation damage, mechanical material properties degradation model due to lightning strike ablation damage was presented based on the method of phenomenological analysis. A 3D progressive damage degradation model with lightning ablation damage on composites was constructed using the method of continuum damage mechanics (CDM), in which Hashin and Yeh delamination failure criteria were employed to verify the occurrence of failure point. According to the model constructed, residual strength of composite coupons with lightning ablation damage under tensile load was predicted through ABAQUS software combining the UMAT subroutine, which was coded by the stiffness matrix progressive damage degradation model. Tensile residual strength simulation accuracy demonstrates the efficiency of the constructed model.

Keywords: Ablation damage; Composite coupons; Tensile residual strength; Influence factors; Lightning strike

收稿日期: 2020-06-09
基金项目: 国家自然科学基金(51476187)
作者简介: 刘远飞(1982—), 男, 空军工程大学航空工程学院机务大队特设队队长兼工程师, 研究领域为飞机与发动机结构、电气设备使用及维护. Email: 68052146@qq.com
通讯作者: 张驭. Email: frank_sharon1314@126.com

1 Introduction

According to the airliner statistics, aircrafts always suffer from lightning strike, the natural phenomena[1-2]. Due to the better mechanical properties and outstanding design characteristics, CFRP (carbon fiber reinforced polymer) composites have been widely used in aerospace[3-4]. However, one of the main drawbacks of composites when compared with traditional metallic materials is the inferior electrical conductivity (1/1000 of aluminum alloy's). Other than metallic structure, when lightning hits composites, the heating, shockwave and magnetic force will cause damages like fiber fracture, resin pyrolysis and delamination, which may decrease performance and result in serious consequence[5].

Currently, researchers have conducted some artificial lightning tests[6-9] and coupled thermal-electrical simulation[10-17] to investigate composite lightning strike thermal ablation damage caused by resisting heat and thermal flux, from the respect of damage mechanism, damage types and damage influence factors, and had got some achievements. Hirano *et al.*[6] investigated the damage behaviors and forming reasons of lightning struck composites. Feraboli *et al.*[7-8] used tests to compare the damages of lightning strike with impact. Ogasawara *et al.*[10], Abdelal *et al.*[11], Wang *et al.*[12] and Dong *et al.*[13-14] studied transient temperature distribution and ablation of CFRP composites based on the proposed models. However, there are few researches on the mechanical properties of composites after lightning strike. With experiments, author in literature [8] did some tests to evaluate the effects of lightning strike damage to composite tension and compression strength. Mall[4] tested the compression strength degradation of the lightning struck nano-composites. Kawakami *et al.*[18] tested the bending residual strength of scarf-repaired mesh-protected composites through four-point bend approach.

According to these existing literatures, there exist rare research about mechanical properties of lightning struck composites by means of finite element model (FEM), and the greatest difficulty encountered during the simulation research is how to characterize composite lightning ablation damage. For the traditional composite low-velocity impact and hygrothermal damage, researchers had put forward several methods to characterize them, such as method of softening inclusion, damage accumulation and equivalent hole. In this paper, for the lightning strike ablation characterization, according to its characterization revealed from experiment, and by the method of phenomenological analysis, we presented that the mechanical material property degradation extent was related to the degree of resin thermal decomposition, and constructed the stiffness matrix progressive damage degradation model of composite laminate with ablation damage. Based on ABAQUS software, simulations for composite laminate with lightning strike ablation were conducted. Then, combining with the UMAT subroutine, which was coded by stiffness matrix progressive damage degradation model, residual strength of compsoite coupons with lightning ablation damage under tensile load was predicted, and the simulation accuracy demonstrates the efficiency of the constructed model.

2 Theory

2.1 Constitutive relationships of materials

The constitutive relationship between stress and strain for orthotropic composite materials has the form:

$$\{\sigma\}=[C]\{\varepsilon\} \tag{1}$$

where: $\{\sigma\}=[\sigma_1\ \ \sigma_2\ \ \sigma_3\ \ \tau_{23}\ \ \tau_{12}\ \ \tau_{13}]^T$; $\{\varepsilon\}=[\varepsilon_1\ \ \varepsilon_2\ \ \varepsilon_3\ \ \gamma_{23}\ \ \gamma_{12}\ \ \gamma_{13}]^T$.

$$[C]=\begin{bmatrix} C_{11} & C_{12} & C_{13} & & & \\ & C_{22} & C_{23} & & & \\ & & C_{33} & & & \\ & & & C_{44} & & \\ & sym & & & C_{55} & \\ & & & & & C_{66} \end{bmatrix} \tag{2}$$

Components in stiffness matrix $[C]$ can be expressed by material properties as follow:

$$C_{11}=\frac{1-\nu_{23}\nu_{32}}{E_2E_3\Delta},C_{12}=\frac{\nu_{21}+\nu_{31}\nu_{23}}{E_1E_3\Delta},$$

$$C_{13}=\frac{\nu_{13}+\nu_{12}\nu_{23}}{E_1E_2\Delta},C_{22}=\frac{1-\nu_{13}\nu_{31}}{E_1E_3\Delta},$$

$$C_{23}=\frac{\nu_{23}+\nu_{21}\nu_{13}}{E_1E_2\Delta},C_{33}=\frac{1-\nu_{12}\nu_{21}}{E_1E_2\Delta},$$

$$C_{44}=G_{23},C_{55}=G_{12},C_{66}=G_{13},$$

$$\Delta=\frac{1-\nu_{12}\nu_{21}-\nu_{23}\nu_{32}-\nu_{13}\nu_{31}-2\nu_{21}\nu_{32}\nu_{13}}{E_1E_2E_3},$$

$$\frac{\nu_{12}}{E_1}=\frac{\nu_{21}}{E_2},\quad\frac{\nu_{13}}{E_1}=\frac{\nu_{31}}{E_3},\quad\frac{\nu_{23}}{E_2}=\frac{\nu_{32}}{E_3}$$

where $E_i(i=1,2,3)$is elastic modulus; ν_{ij} $(i=1,2,3;j=1,2,3;i\neq j)$ is Poisson's ratio; G_{23}, G_{31}, $G_{12}$are shear modulus.

2.2 Lightning strike ablation damage of composite laminates

2.2.1 Material property degradation model with lightning strike ablation　During lightning strike, temperature at lightning strike attachment point and nearby region will increase rapidly due to the act of resistive heating. Once the resin thermal decomposition temperature is satisfied, it will be decomposed gradually accompany with the increasing temperature. When the degree of decomposition is limited, composite material properties change little, and accompany with the thermal decomposition of resin, material properties descend gradually. Once resin decompose completely, we can also assume that the composite material properties degrade completely, and then, it cannot bear load any more. It can be explained through the point of view: in the territory with resin decompose completely, the internal resin decomposed gases will expand rapidly, under the act of which the bareness carbon fiber is fractured, and sketch map is shown in Fig. 1. Based on the above perspective, we put forward the material property degradation model due to lightning strike ablation damage as follow: when the temperature is lower than the thermal decomposition initial temperature, composite material properties remain the same as origin; when the temperature locates in the range of the thermal decomposition temperature, composite material properties change linearly with the degree of decomposition; when the temperature is higher than the thermal decomposition termination temperature, composite material properties are zero, but for the sake of improving the convergence of simulation, we assumed that the composite material properties are 0.001 times as much as the initial material properties.

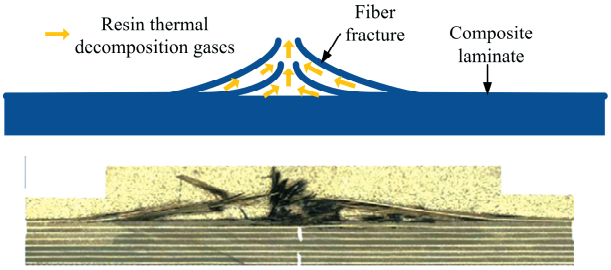

Fig. 1　Fractured carbon fiber under the act of resin thermal decomposition gases

Set parameter K as the composite initial material property (elastic modulus and shear modulus change with the degree of decomposition would be taken into account), and t_0 is the thermal decomposition initial temperature; t_1 is the thermal decomposition termination temperature. During the whole temperature rising process, composite material properties can be expressed as:

$$K=\begin{cases}K, & (t\leqslant t_0)\\(1-\alpha(T))K, & (t_0<t\leqslant t_1)\\0.001K, & (t>t_1)\end{cases}\tag{3}$$

where $\alpha(T)$ denotes resin decomposition degree, and temperature T determines the rate of the decomposition. For thermosetting resin, the decomposition kinetics can be estimated as[19]

$$\frac{\mathrm{d}\alpha}{\mathrm{d}T}=\frac{A}{\beta}\exp(-\frac{E_a}{RT})(1-\alpha)^n\tag{4}$$

where A is pre-exponential factor, β is constant heating rate, E_a is activation energy, R (8.314 J/mol/K) is universal gas constant and n is reaction order.

By separation of the variables[20],

$$g(\alpha)=\int_0^\alpha\frac{\mathrm{d}\alpha}{(1-\alpha)^n}=\frac{A}{\beta}\int_{t_0}^{t_1}\exp(-\frac{E_a}{RT})\mathrm{d}T\tag{5}$$

then

$$\alpha=1-\exp\left[\frac{1}{1-n}\ln\left\{1-(1-n)\int_{t_0}^{t}\frac{A}{\beta}\exp(-\frac{E_a}{RT})\mathrm{d}T\right\}\right]\tag{6}$$

Thus, with a temperature function, the decomposition degree can be shown.

2.2.2 Characterization of lightning strike ablation damage The existence of ablation damage will induce the degradation of material properties, and chapter 2.2.1 gave the material properties degradation model due to the ablation damage. Thus, according to phenomenological analysis method, the lightning strike ablation can be characterized based on constructing the stiffness matrix progressive damage degradation model of composite laminate with ablation damage. Set matrix $[C^{d,s}]$as the stiffness matrix of composite laminate with ablation damage, combing Eq. (2) and Eq. (3), it can be expressed as:

$$[C^{d,s}]=\begin{cases}[C], & (t\leqslant t_0)\\ (1-\alpha(T))[C], & (t_0<t\leqslant t_1)\\ 0.001[C], & (t>t_1)\end{cases} \tag{7}$$

In order to keep the material properties at temperature t_1 consist with the material properties when temperature higher than t_1, maximum value of $\alpha(T)$ is 0.999.

2.3 Composite laminate progressive damage analysis based on CDM

2.3.1 Damage characterization First, the material coordinate system is defined: 1 represents the longitudinal direction of the fiber; 2 and 3 indicate the transverse directions of the fibers. Here we adapt a second-order symmetric tensor D to define material damage, its eigenvalues $d_i(i=1,2,3)$represent the descending degree of the effective bearing area on the three main directions, which also can represent the damage variables for the delamination. The value of damage variables d_i must be in the range of 0 to 1, where $d_i=0/1$ denotes the perfect/complete-damaged material[21].

$$D=\begin{bmatrix}d_1 & 0 & 0\\ 0 & d_2 & 0\\ 0 & 0 & d_3\end{bmatrix} \tag{8}$$

Based on CDM analysis method, once the material occur damage, the effective stress $[\bar{\sigma}]$ can be expressed by the nominal stress $[\sigma]$ as

$$[\bar{\sigma}]=M(D)[\sigma] \tag{9}$$

where $M(D)$ is damage operator, and

$$M(D)=\mathrm{diag}\left[\frac{1}{k_{11}}\quad\frac{1}{k_{22}}\quad\frac{1}{k_{33}}\quad\frac{1}{k_{23}}\quad\frac{1}{k_{12}}\quad\frac{1}{k_{13}}\right]$$

$$k_{ij}=\sqrt{(1-d_i)(1-d_j)}\quad(i,j=1,2,3) \tag{10}$$

By the energy equivalence assumption,

$$W^e=\frac{1}{2}[\sigma][\varepsilon]=\frac{1}{2}[\bar{\sigma}][\bar{\varepsilon}] \tag{11}$$

where W^e is the elastic strain energy density; $[\bar{\varepsilon}]$ and $[\varepsilon]$ are the effective strain and the nominal strain, respectively.

Taking Eq. (9) into Eq. (11), the elastic strain energy density is

$$W^e=\frac{1}{2}M(D)^{-1}[\bar{\sigma}][\varepsilon]=\frac{1}{2}[\bar{\sigma}][\bar{\varepsilon}] \tag{12}$$

According to Eq. (12), we can get the relationship between the effective strain and the nominal strain:

$$[\bar{\varepsilon}]=M(D)^{-1}[\varepsilon] \tag{13}$$

Using $[C^d]$ to present the stiffness matrix of damage material, and combing Eq. (1), Eq. (12) and Eq. (13), $[C^d]$ has the form:

$$[C^d]=M(D)^{-1}[C](M(D)^T)^{-1} \tag{14}$$

2.3.2 Initial failure criteria Hashin[22] and Yeh delamination failure criteria[23] were employed to verify the occurrence of a failure point. F_1, $F_2$and F_3 were adopted to describe the initial failure criteria of fiber, resin and delamination respectively. When composite laminate has internal damage, the stresses in local damage territory distribute complexly and change violently. However, the strains' distribution changes continuously and smoothly, thus, initial failure criteria based on effective strains is more suitable for describing the progressive damage evolution of composite structure. Without regard to the condition of shear nonlinearity, Hashin and Yeh delamination failure criteria have the following general forms based on the effective strains[24]:

$$F_1^2=\begin{cases}\left(\frac{\varepsilon_{11}}{\varepsilon_1^{f,T}}\right)^2+\left(\frac{\gamma_{12}}{\gamma_{12}^f}\right)^2+\left(\frac{\gamma_{13}}{\gamma_{13}^f}\right)^2\geqslant 1, & (\varepsilon_{11}>0)\\ \left(\frac{\varepsilon_{11}}{\varepsilon_1^{f,C}}\right)^2\geqslant 1, & (\varepsilon_{11}<0)\end{cases} \tag{15}$$

$$F_2^2=\begin{cases}\left(\frac{\varepsilon_{22}+\varepsilon_{33}}{\varepsilon_2^{f,T}}\right)^2+\frac{1}{(\gamma_{23}^f)^2}(\gamma_{23}^2-\frac{E_2E_3}{G_{23}^2}\varepsilon_{22}\varepsilon_{33})+\\ \left(\frac{\gamma_{12}}{\gamma_{12}^f}\right)^2+\left(\frac{\gamma_{13}}{\gamma_{13}^f}\right)^2\geqslant 1,\ (\varepsilon_{22}+\varepsilon_{33}>0)\\ \left(\frac{E_2\varepsilon_{22}+E_3\varepsilon_{33}}{2G_{12}\gamma_{12}^f}\right)^2+\left(\frac{\varepsilon_{22}+\varepsilon_{33}}{\varepsilon_2^{f,C}}\right)\left[\left(\frac{E_2\varepsilon_2^{f,C}}{2G_{12}\gamma_{12}^f}\right)^2-1\right]+\\ \frac{1}{(\gamma_{23}^f)^2}(\gamma_{23}^2-\frac{E_2E_3}{G_{23}}\varepsilon_{22}\varepsilon_{33})+\\ \left(\frac{\gamma_{12}}{\gamma_{12}^f}\right)^2+\left(\frac{\gamma_{13}}{\gamma_{13}^f}\right)^2\geqslant 1,\ (\varepsilon_{22}+\varepsilon_{33}<0)\end{cases} \tag{16}$$

$$F_3^2=\begin{cases}\left(\frac{\varepsilon_{33}}{\varepsilon_3^{f,T}}\right)^2+\left(\frac{\gamma_{13}}{\gamma_{13}^f}\right)^2+\left(\frac{\gamma_{23}}{\gamma_{23}^f}\right)^2\geqslant 1,\ (\varepsilon_{33}>0)\\ \left(\frac{\gamma_{13}}{\gamma_{13}^f}\right)^2+\left(\frac{\gamma_{23}}{\gamma_{23}^f}\right)^2\geqslant 1,\ (\varepsilon_{33}<0)\end{cases} \tag{17}$$

In the above equations, $\varepsilon_{ii}(i=1,2,3)$ is the normal strain in i direction; γ_{12}, γ_{13} and γ_{23} are the shear strains in 1-2, 1-3 and 2-3 planes, respectively. $\varepsilon_i^{f,T}$ or $\varepsilon_i^{f,C}(i=1,2,3)$ represents tensile or compressive normal strain strength in i direction, γ_{12}^f, γ_{13}^f and γ_{23}^f denote shear strain strength in 1-2, 1-3 and 2-3 planes:

$$\varepsilon_1^{f,T}=\frac{X_T}{C_{11}},\ \varepsilon_1^{f,C}=\frac{X_C}{C_{11}},$$

$$\varepsilon_2^{f,T}=\frac{Y_T}{C_{22}},\ \varepsilon_2^{f,C}=\frac{Y_C}{C_{22}},$$

$$\varepsilon_3^{f,T}=\frac{Z_T}{C_{33}},\ \varepsilon_3^{f,C}=\frac{Z_C}{C_{33}},$$

$$\gamma_{12}^f=\frac{S_{12}}{C_{44}},\ \gamma_{13}^f=\frac{S_{13}}{C_{55}},\ \gamma_{23}^f=\frac{S_{23}}{C_{66}}$$

2.3.3　Damage evolution　In the initial failure criteria, when F_i is less than 1, the material is non-damaged. When F_i equal to 1, the material is damaged, and any further loading will cause the degradation of material stiffness coefficients, and at this time, by adopting the degradation model of material properties based on exponential material damage evolution law, calculation formula for damage state variables can be described as[25]:

$$d_i=1-\frac{\exp(C_{ii}(\varepsilon_i^f)^2L^c(1-F_i)/G_i^C}{F_i},\quad i=1,2,3 \tag{18}$$

where L^c is the characteristic length of the FE, which can reduce the mesh sensitivity during the stage of damage evolution; G_i^C denotes the critical fracture dissipation energies in the three main material directions, respectively.

3　Experimental and analytical approach

3.1　Experimental approach

3.1.1　Material and specimen preparation　Aircraft typical carbon woven fabric/epoxy (CCF300/5228A) laminates were tested, and the portion of carbon fibers is approximate to 55%. The test coupons were designed according to GB/T3354-2014[26], with its dimension 90 mm×44 mm×4 mm. Each coupon has 16 plies (0.25 mm) carbon woven fabrics, and the ply orientation angle is [(0/90F)]. Its mechanical and electrical/thermal material properties at room temperature are listed in Tab. 1 and Tab. 2.

Tab. 1　Mechanical material properties of CCF300/5228A composites

E_1/GPa	E_2/GPa	E_3/GPa	ν_{12}	ν_{13}	ν_{23}	G_{12}/GPa	G_{13}/GPa	G_{23}/GPa	X_T/MPa	X_C/MPa
70	70	7.6	0.044	0.45	0.45	6.3	4	4	680	650
Y_T/MPa	Y_C/MPa	Z_T/MPa	Z_C/MPa	S_{12}/MPa	S_{13}/MPa	S_{23}/MPa	G_1^CN/mm	G_2^CN/mm	G_3^CN/mm	η
680	650	58	165	100	65	65	12.5	1	1	1e-6

Tab. 2　Electrical/thermal material properties of CCF300/5228A composites[27]

Density/(kg/mm³)	Specific heat/(J/kg℃)	Thermal conductivity/(W/mm℃)		Electrical conductivity/(S/m)	
		Longitudinal/Transverse	In depth	Longitudinal/Transverse	In depth
1.52e-6	1 065	0.008	0.000 67	32 500	3.25e-2

3.1.2　Artificial lightning testing　Impulse current generator for lighting test is shown in Fig. 2 (a). For less contact resistance, test specimens should be fixed in the test jig completely. The

specimens have the same electric potential, and conductive silver sol and copper foil are covered on the surfaces. The copper probe locates upon the center of the specimens and the distance is 1 mm.

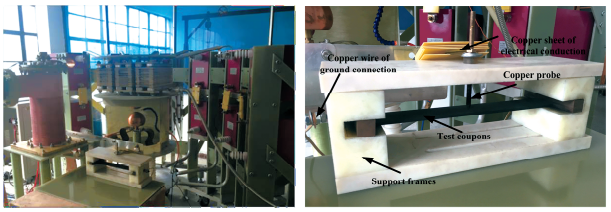

(a) Impulse current generator (b) Test jig

Fig. 2 Images of lightning strike test equipment

From SAE ARP 5412A[28], the four waveforms (A-D) are shown in Fig. 3, and A, D are always chosen for lightning strike tests because of their higher peak current. For the current components, the double exponential equation is

$$i(t)=I_0(e^{-\alpha t}-e^{-\beta t}) \tag{19}$$

where I_0 is current constant, α and β are the reciprocal values of wave tail and front time constants. For the expression of current waveform with the double exponential equation, T_1 and T_2 are introduced, where T_1 is the maximum current arrival time, T_2 is the arrival time at 50% of the maximum current.

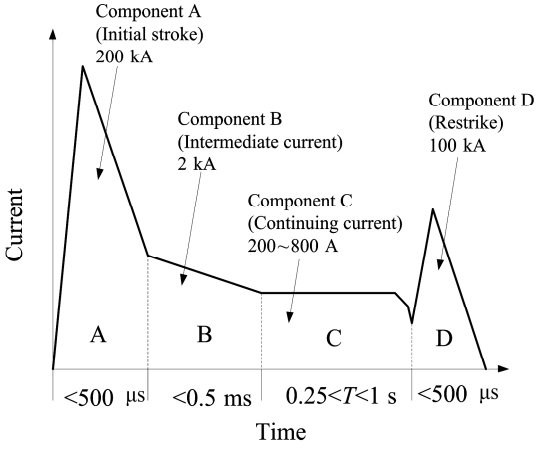

Fig. 3 Simulated normative lightning current waveforms

Component D, the restrike of lightning infliction, was set for the test, and the conditions, parameters are shown in Tab. 3.

3.1.3 Tensile residual strength testing The apparatus of tension test is MTS 880~500 kN. In this paper, tensile residual strength test specimens were divided into two groups: one is tensile test for un-damaged composite coupons, numbering S0-1~S0-3; and the other one is tensile test for post-lightning composite coupons, which is shown in Tab. 3. Tensile test was carried out according to GB/T 3354-2014, four aluminium strengthening plates were bonded to each specimen tension face before test. Application of tensile load was adopted by the displacement-controlled manner, and loading rate was 1.5 mm/min, recording the load-displacement curves during the whole test.

Tab. 3 The conditions and lightning strike parameters in the test

Test condition	T_1/ T_2 /μs	Peak current /kA	Action integral/A^2s	Numbering
1	5.03/19.37	30.58	12 615	S1~S3
2	5.14/19.47	51.42	35 270	S4~S6
3	5.18/21.37	80.16	97 233	S7~S9

3.2 Finite-element models

In order to predict the tensile residual strength of composite coupons with lightning ablation using FEM method, the analysis process can be divided into two steps: first, when lightning strike, the transient temperature field was obtained by ABAQUS and the thermal decomposition behavior of resin was combined to simulate composite lightning strike ablation damage due to resistance heating; second, based on ABAQUS/Standard and combining UMAT user subroutine coded by stiffness matrix progressive damage degradation model, residual strength was predicted under tensile load for composite laminate with lightning strike ablation damage, and during this step, the transient temperature field result in first step was regarded as the predefined temperature field.

For the same type composite coupons in this paper, its lightning strike ablation damage analysis mathematical model and FEM were detailed shown in reference[27, 29], and the relative theory and method will not be restated here. Material thermal/electrical properties under different temperatures were shown in reference[27].

According to the method introduced in literature[27, 29], FE model is established according to the test specimens, and the length = 290 mm, the width = 44 mm (Fig. 4), and the electrical currents (in Tab. 3) were injected strictly into the model.

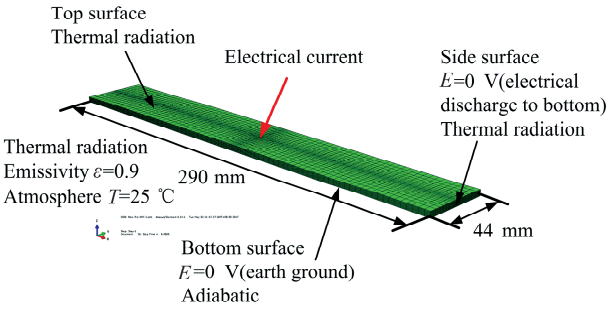

Fig. 4　Composite FE model exposed to simulated lighting current

For the assessment of the tensile residual strength of composite coupons with lightning strike ablation damage based on ABAQUS/Standard, element type was C3D8R. One side of the coupon was fixed and the other one applied a displacement load as the boundary conditions. The transient temperature field result got by the coupled thermal-electrical analysis was regarded as predefined temperature field. By combing UMAT user subroutine, the tensile residual strength was calculated.

4　Results and discussion

4.1　Comparison between FEM and experimental results

To verify the accuracy of the simulation results, tensile residual strength comparison between FEM and experiment are shown in Tab. 4. According to Tab. 4, we can see that the compared errors of tensile residual strength between test results and simulation results under different peak current are all less than 4%.

Fig. 5 shows the tensile damage mode compared results between FEM and experiment, including un-damaged composite coupons and composite coupons with lightning ablation (Fig. 5). The tensile damage mode simulation results is in accordance with experiment well, for un-damaged composite coupons, under tensile load, its failure location locates at both ends of the coupons; but for composite coupons with lightning ablation damage, its failure location locates at the ablation damage territory of the coupons. As a result, the model established in this paper is applicable.

Tab. 4　Tensile residual strength in the experiment and simulation

Peak current /kA	Experimental average tensile residual strength/kN	Simulation tensile residual strength/kN	E_{rror}/%
0	118.5	115	−2.95
30.58	106.7	102.7	−3.74
51.42	95.47	93.52	−2.04
80.16	87.70	88.65	1.08

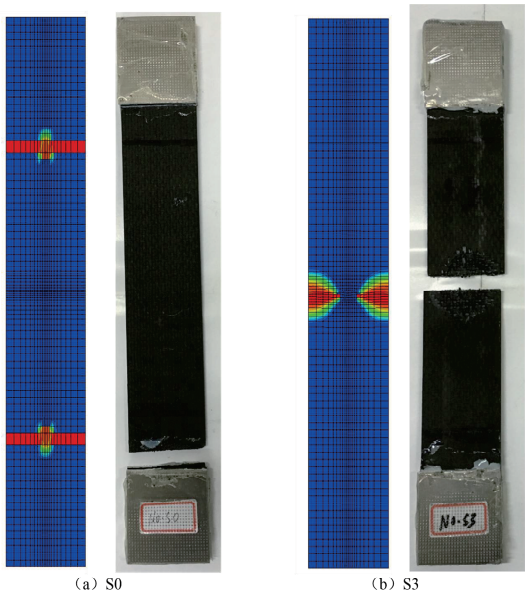

(a) S0　　(b) S3

Fig. 5　Damage mode compared between experiment and simulation

4.2　Tensile residual strength influence factors analysis for post-lightning coupons

4.2.1　Influence of lightning current parameters on tensile residual strength　According to literature[29], lightning current parameter such as charge transfer and action integral could be introduced for composite lightning strike ablation characterization, and power function exists for both the parameters above and the ablation damage. In this paper, based on the tensile residual strength prediction FEM model, the influence of lightning current parameters on the degradation extent of composite coupons tensile strength was

investigated, which verifies the characterization parameters of tensile residual strength. Tab. 5 shows the lightning current analyzed parameters and their corresponding tensile residual strength simulation results.

The influence of charge transfer and action integral on tensile residual strength of composite coupons are shown in Fig. 6. According to the scatter points change trend, with increase of the two lightning current parameters, tensile residual strength decreased. To study the relationship between lightning current parameters above and tensile residual strength, regression of the degradation extent of composite coupons tensile strength and lightning current parameters above were investigated based on the power function, red curves in Fig. 6 represent the fitting curves, and the fitting results are shown in Tab. 6, in which we can see that, both the charge transfer and the action integral show power function with tensile residual strength, but when compared the related indexes R^2 got in Tab. 6 between the charge transfer and the action integral, under the power function, the related indexes R^2 of the charge transfer is 0.888 3, and that of the the action integral is 0.987 7, so the compared results indicate that the action integral could be the better degradation extent characterization.

Tab. 5 Relationship between tensile residual strength and lightning current parameters

$T_1/T_2/\mu s$	Peak current /kA	Charge transfer/C	Action integral/(A^2s)	Load /kN
2.6/10.5	10	0.121	867.5	112.97
	30	0.363	7 807.5	99.86
	50	0.605	21 687.5	97.58
	80	0.968	55 520	90.45
4/20	10	0.240	1 700	107.76
	30	0.720	15 300	98.00
	50	1.200	42 500	94.35
	80	1.920	108 800	89.11
5/28	10	0.377 5	2 587.5	107.61
	30	1.132 5	23 287.5	96.57
	50	1.887 5	64 687.5	90.13
	80	3.02	165 600	86.53
6/69	10	0.83	5 875	102.21
	30	2.49	52 875	91.88
	50	4.15	146 875	88.52
	80	6.64	376 000	84.42

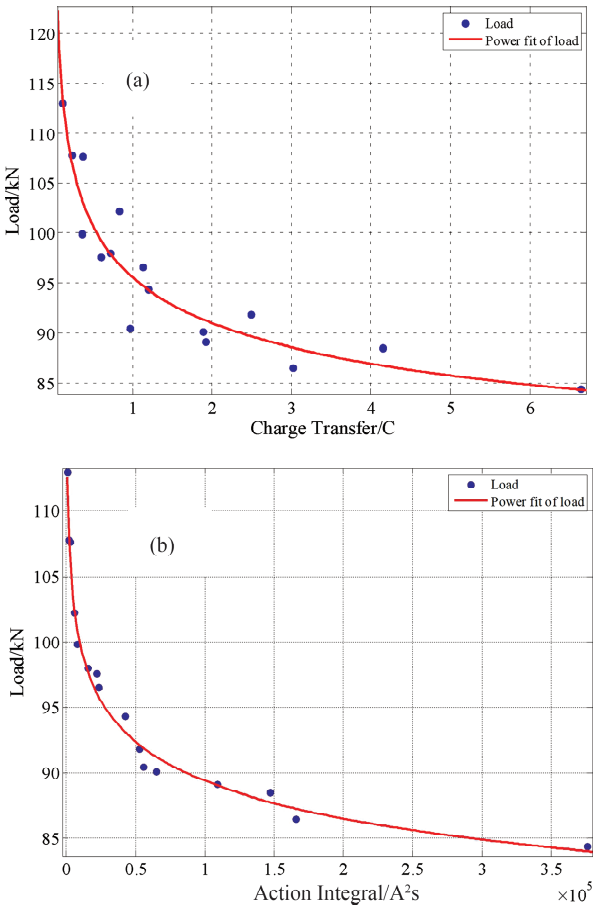

Fig. 6 Effects of charge transfer (a) and action integral (b) on tensile residual strength

Tab. 6 Fitting results between lightning current parameters and tensile residual strength

Fitting function	$f(x)=a\times x^b+c$(x represent charge transfer and action integral)			Related indexes
Fitting parameters	a	b	c	R^2
Charge transfer	38.85	−0.1808	56.72	0.8883
Action integral	140.3	−0.06001	19.08	0.9877

From Fig. 6, it can be easily seen that when the composite was subjected to a relatively small intensity of the lightning current (action integral less than 5 000 A^2s), the decrease rate of the tensile residual strength of composite coupons was quick, and with the increase of lightning current intensity, tensile residual strength decrease rate became slower. According to the damage extent induced by lightning current, when the lightning

current intensity was less than a certain degree, the lightning damage would be confined within the width of the coupons, right now, energy of the lightning current was mainly consumed by forming lightning damage, and the area and depth of the lightning damage increased quick. Therefore, tensile residual strength of composite coupons with lightning ablation damage decreased quick first. However, when the lighting current was higher than the certain value, lightning damage would be outside of the width of the coupons, because the lightning damage territory had a higher electrical conductivity due to high temperature, combined with the boundary conditions of FEM, lightning damage territory would form a steady current conduction channel along the width direction of the coupon, and a lot of lightning current will be conducted away through the channel, at this time, new lightning damage would be hardly formed, especially in the thickness direction, thus, tensile residual strength of composite coupons with lightning ablation damage decreased smoothly. In literature [29], relationships between action integral and lightning damage area and depth were clarified, and the same results as analysis above were shown.

4.2.2 **Influence of thermal/electrical properties on tensile residual strength** According to literature[29], thermal conductivity of the composite will also hardly affect the tensile residual strength of composite coupons with lightning ablation damage. Therefore, in this paper, we are mainly focus on the effects of composite electrical conductivity and specific heat on the degradation extent of composite coupons tensile strength. When simulating, the lightning current waveform remained 6/69 μs and the peak current reached 80 kA. Tab. 5 shows the tensile residual strength under this lightning parameter when composite coupon had the original thermal/electrical properties.

Fig. 7 shows the simulation tensile displacement-load curves of composite with lightning ablation damage under different electrical conductivity and specific heat. From Fig. 7 (a), during the increasing of electrical conductivity from 3.25×10^4 S/m to 3.25×10^7 S/m, tensile residual strength of composite coupons with lightning ablation damage increased obviously. If the electrical conductivity was double, treble and quadruple of the original, tensile residual strength were 90.45, 105.32 and 110.3 kN respectively, and compared with that of original electrical conductivity, the tensile residual strength respectively increased by 7.14%, 24.76% and 30.66%. According to the simulation results in Tab. 4, tensile strength of the undamaged composite coupon was 115 kN, thus, if the electrical conductivity was double, treble and quadruple of the original, the corresponding tensile residual strength kept 78.65%, 91.58% and 95.91% than that of the undamaged composite coupon, visibly, if the electrical conductivity was higher than the treble, tensile residual strength would keep higher than 90% than that of its undamaged state. From Fig. 7 (b), during the increasing of specific heat from 1 065 to 10 650 J/kg℃, tensile residual strength of composite coupons with lightning ablation damage increased also. When the specific heat were two, five and ten times than the original, tensile residual strength were 87.50, 88.52 and 91.44 kN respectively, compared with that of original specific heat, the tensile residual strength respectively increased by 3.65%, 4.86% and 8.32%, and compared with the undamaged composite coupon, when the specific heat were two, five and ten times than the original, the corresponding tensile residual strength kept 76.09%, 76.91% and 79.51% than that of the undamaged composite coupon.

The tensile residual strength of composite coupons with lightning strike ablation damage under different electrical conductivity and specific heatwere simulated, then after regression analyzing, Fig. 8 shows the fitting curves of tensile residual strength, power function was selected as the analysis function, and mathematical model between tensile residual strength and electrical con-

ductivity and specific heat were been constructed, as is shown in Tab. 7, the related indexes R^2 between tensile residual strength with electrical conductivity and specific heat were 0.9605 and 0.946 2 respectively.

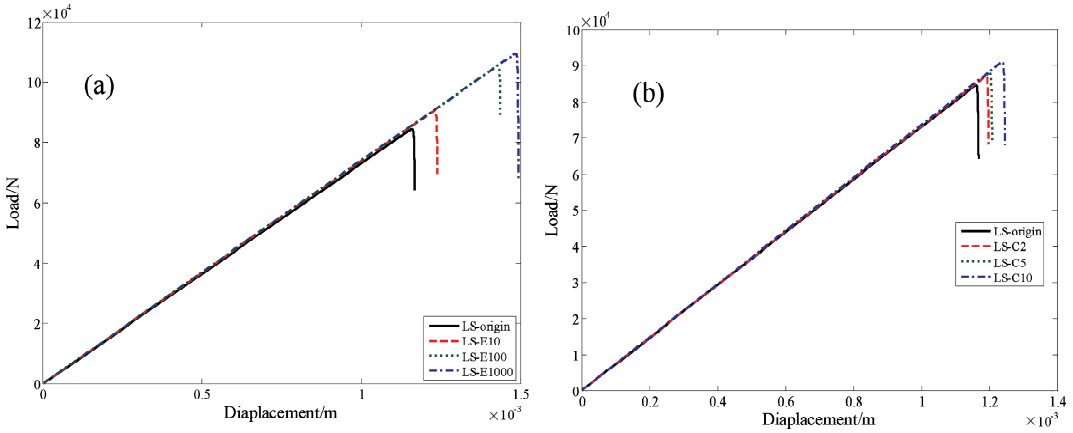

Fig. 7 Tensile displacement-load curves under different electrical conductivity (a) and specific heat (b)

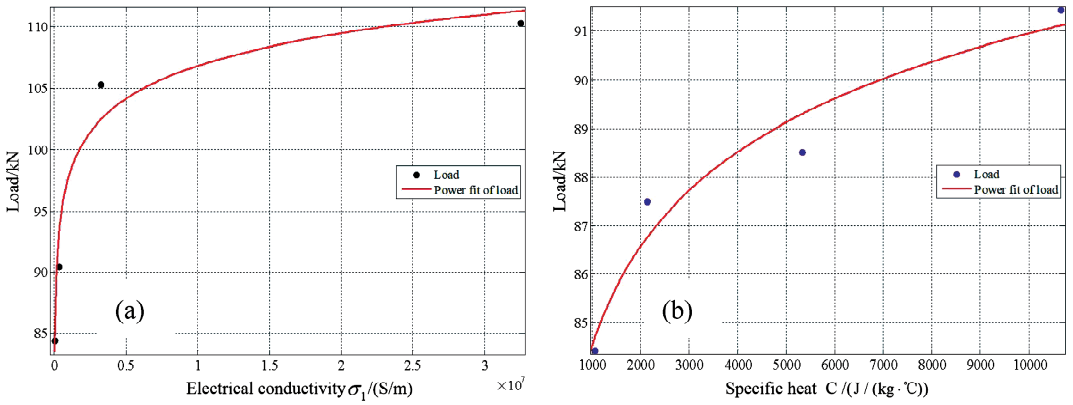

Fig. 8 Effects of electrical conductivity (a) and specific heat (b) on tensile residual strength

Tab. 7 Fitting results between material electrical/thermal properties and tensile residual strength

Fitting function	$f(x)=a\times x^b+c$(x represent electrical conductivity and specific heat)			Related indexes
Fitting parameters	a	b	c	R^2
Electrical conductivity	−259.3	−0.02059	292.9	0.9605
Specific heat	−68.76	−0.07343	125.9	0.9462

Thus, by means of enhancing the composite electrical conductivity and specific heat, tensile residual strength of composite coupons with lightning ablation damage could be increased distinctly. Furthermore, influence of enhancing electrical conductivity on enhancing tensile residual strength was most remarkable, and if the electrical conductivity was higher than the treble, tensile residual strength would keep higher than 90% than that of its undamaged state.

5 Conclusions

By the means of phenomenological analysis, material properties degradation model due to lightning strike ablation damage was presented to characterizing composite lightning ablation damage. A 3D progressive damage degradation model for composite with lightning ablation damage was constructed by the method of continuum damage mechanics (CDM), based on that residual strength of composite coupons with lightning ablation damage under tensile load was predicted through ABAQUS software and UMAT subroutine, which was coded by the stiffness matrix progressive damage degradation model. The accuracy of FEM was verified with the comparison of composite tensile experimental data from residual

strength and damage mode.

Influence of lighting current parameters and thermal/electrical properties of composite on degradation extent of composite coupons tensile strength were simulated and analyzed. It is shown that tensile residual strength of composite coupons with lightning strike ablation is distinctly influenced by lightning current charge transfer and action integral, and there exists strong power function between tensile residual strength and action integral, and with comparison of charge transfer and action integral, action integral could be used for the degradation extent characterization better. Composite own thermal/electrical material properties, such as electrical conductivity and specific heat, could affect the tensile residual strength. When the lightning current parameters are constant, if the electrical conductivity was double, treble and quadruple of the original, the tensile residual strength respectively increased by 7.14%, 24.76% and 30.66% , and the corresponding tensile residual strength kept 78.65%, 91.58% and 95.91% than that of the undamaged composite coupon, visibly, if the electrical conductivity was higher than the treble, tensile residual strength would keep higher than 90% than that of its undamaged state. When the specific heat were two, five and ten times than the original, the tensile residual strength respectively increased by 3.65%, 4.86% and 8.32%, and the corresponding tensile residual strength kept 76.09%, 76.91% and 79.51% than that of the undamaged composite coupon. So there exists strong power function relationship between tensile residual strength and thermal/electrical parameters.

References:

[1] Uman M A, Rakov V A. The interaction of lightning with airborne vehicles [J]. Prog Aerosp Sci, 2003, 39: 61.

[2] Gagné M, Therriault D. Lighting strike protection of composites [J]. Prog Aerosp Sci, 2014, 64: 1.

[3] Georgiadis S, Gunnion A J, Thomson R S, *et al*. Bird-strike simulation for certification of the Boeing 787 composite moveable trailing edge [J]. Compos Struct, 2008, 86: 258.

[4] Mall S. Compression strength degradation of nanocomposites after lightning strike [J]. J Compos Mater, 2009, 43: 2987.

[5] Rupke E. Lightning direct effects handbook [M/OL]. Pittsfield: Lightning Technologies Inc., 2002 [2020-06-07]. http://www.doc88.com/p-870818713674.html.

[6] Hirano Y, Katsumata S, Iwahori Y, *et al*. Artificial lighting on graphite/epoxy composite laminate [J]. Compos Part A, 2010, 41: 1461.

[7] Feraboli P, Kawakami H. Damage of carbon/epoxy composite plates subjected to mechanical impact and simulated lightning [J]. J Aircr, 2010, 47: 999.

[8] Feraboli P, Miller M. Damage resistance and tolerance of carbon/epoxy composite coupons subjected to simulated lightning strike [J]. Compos Part A, 2009, 40: 954.

[9] Li Y C, Li R F, Lai H. Effect of hygrothermal aging on the damage characteristics of carbon woven fabric/epoxy laminates subjected to simulated lightning strike [J]. Mater Design, 2016, 99: 477.

[10] Ogasawara T, Hirano Y, Yoshimura A. Coupled thermal-electrical analysis for carbon fiber/epoxy composites exposed to simulated lighting current [J]. Compos Part A, 2010, 41: 973.

[11] Abdelal G, Murphy A. Nonlinear numerical modeling of lightning strike effect on composite panels with temperature dependent material properties [J]. Compos Struct, 2014, 109: 268.

[12] Wang Y, Zhupanska O I. Lightning strike thermal damage model for glass fiber reinforced polymer matrix composites and its application to wind turbine blades [J]. Compos Struct, 2015, 132: 1182.

[13] Dong Q, Guo Y L, Sun X C. Coupled electrical-thermal-pyrolytic analysis of carbon fiber/epoxy composites subjected to lightning strike [J]. Polymer, 2015, 56: 385.

[14] Dong Q, Guo Y L, Chen J L. Influencing factor analysis based on electrical-thermal-pyrolytic simulation of carbon fiber composites lightning damage [J]. Compos Struct, 2016, 140: 1.

[15] Wang F S, Ding N, Liu Z Q, *et al*. Ablation damage characteristic and residual strength prediction of carbon fiber/epoxy composite suffered from lightning strike [J]. Compos Struct, 2014, 117: 222.

[16] Li S L, Yin J J, Yao X L. Damage analysis for carbon fiber/epoxy composite exposed to simulated lighting current [J]. J Reinf plast comp, 2016, 35: 1201.

[17] Yin J J, Li S L, Chang F. Ablation damage characteristic analysis of composite laminate with fastener subjected to lightning strike [J]. Appl Compos Mater, 2016, 23: 821.

[18] Kawakami H, Feraboli P. Lightning strike damage resistance and tolerance of scarf-repaired mesh-protected carbon fiber composites [J]. Compos Part A, 2011, 42: 1247.

[19] Bai Y, Keller T, Vallee T. Modeling of thermophysical properties and thermal responses for FRP composites in fire[C]//Asia-pacific conference on FRP in structures. Hong Kong: [s. l.], 2007.

[20] Lee J H, Kim K S, Kim H. Determination of kinetic parameters during the thermal decomposition of epoxy/carbon fiber composite material [J]. Korean J Chem Eng, 2013, 30: 955.

[21] Wang Y, Tong M, Zhu S. Three dimensional continuum damage mechanics model of progressive failure analysis in fiber-reinforced composite laminates [C]//50th AIAA/ASME/ASCE/AHS structures, structure dynamics, and materials conference. California: Palm Springs, 2009.

[22] Hashin Z. Failure criteria for unidirectional fiber composites [J]. J Appl Mech, 1980, 47: 329.

[23] Yeh H Y, Kim C H. The Yeh-Stratton criterion for composite materials [J]. J Compos Mater, 1994, 28: 926.

[24] Huang C H, Lee Y J. Experiments and simulation of the static contact crush of composite laminated plates [J]. Compos Struct, 2003, 61: 265.

[25] MaimiP, Camanho P P, Mayugo J A. A continuum damage model for composite laminates: Part II-Computational implementation and validation [J]. Mech Mater, 2007, 39: 909.

[26] Test method for tensile properties of orientation fiber reinforced polymer matrix composite materials: GB/T 3354-2014 [S]. China: SAC, 2015.

[27] Yin J J, Chang F, Li S L, *et al*. Experimental and numerical simulation analysis of typical carbon woven fabric/epoxy laminates subjected to lightning strike [J]. Appl Compos, 2017, 24: 1353.

[28] Aircraft lightning environment and related test waveforms: SAE-ARP-5412A [S]. USA: SAE, 2005.

[29] Yin J J, Chang F, Li S L, *et al*. Lightning strike ablation damage influence factors analysis of carbon fiber/epoxy composite based on coupled electrical-thermal simulation [J]. Appl Compos, 2016, 24: 1089.

引用本文格式:

中 文: 刘远飞, 张驭, 尹俊杰, 等. 雷击作用下复合材料层合板的烧蚀损伤表征及剩余强度影响因素分析[J]. 四川大学学报: 自然科学版, 2020, 57: 1165.

英 文: Liu Y F, Zhang Y, Yin J J, *et al*. Ablation damage characterization and tensile residual strength influence factors analysis for composite coupons subjected to lightning strike [J]. J Sichuan Univ: Nat Sci Ed, 2020, 57: 1165.